11 May 2000

PHYSICS LETTERS B

ELSEVIER

Physics Letters B 480 (2000) 239–244

Search for ternary fragmentation in the reaction 856 MeV ^{98}Mo + ^{51}V: kinematic probing of intermediate-mass-fragment emissions

Emanuele Vardaci [a,1], Morton Kaplan [a], Winifred E. Parker [a,2], David J. Moses [a,3], J.T. Boger [b,4], G.J. Gilfoyle [c], M.A. McMahan [d], M. Montoya [a]

[a] *Department of Chemistry, Carnegie Mellon University, Pittsburgh, PA 15213-2683, USA*
[b] *Department of Chemistry, State University of New York, Stony Brook, NY 11794-3400, USA*
[c] *Department of Physics, University of Richmond, Richmond, VA 23173, USA*
[d] *Lawrence Berkeley National Laboratory, Berkeley, CA 94720, USA*

Received 27 September 1999; received in revised form 23 March 2000; accepted 27 March 2000
Editor:V. Metag

Abstract

A new technique has been applied to coincidence measurements between fission fragments (FF) and intermediate mass fragments (IMF) emitted from the composite system $^{149}_{65}$Tb at an excitation energy of 224 MeV. The method permits simultaneous observation of IMF emissions along and normal to the FF separation axes. For the integrated total of 0.10 ± 0.02 IMF emitted per fission, we find no significant correlation with FF direction, suggesting that IMFs associated with fission reactions are predominantly emitted from the system prior to fission.

PACS: 25.70.-z; 25.70.Jj; 25.85.-w; 25.85.Ge
Keywords: Heavy ion reactions; Intermediate mass fragments; Fission

Many studies utilizing heavy-ion-induced nuclear reactions have probed various aspects of the formation and decay of the composite nuclear system $^{149}_{65}$Tb, as representative of the behavior of nuclear matter at high excitation energy and angular momentum [1–9]. Produced via several different entrance channels, the ^{149}Tb* de-excitation modes involving fission [1,8], light-charged-particle (lcp) evaporation [1,2,8,9], and intermediate-mass-fragment (IMF) emission [3–7] have been investigated in the excitation energy range $E^* = 130$–240 MeV. The present work was undertaken to address the origins of IMF production by employing a new kinematic technique, to be described below, and to determine if ternary

[1] Present address: Dipartimento di Scienze Fisiche, Universita' di Napoli Federico II, 80126 Naples, Italy.
[2] Present Address: Lawrence Livermore National Laboratory, Livermore, CA 94551.
[3] Present Address: Gaussian, Inc., Carnegie, PA 15106.
[4] Present Address: Brookhaven National Laboratory, Upton, NY 11973.

0370-2693/00/$ - see front matter
PII: S0370-2693(00)00407-X

fragmentation, or IMF emission from the ''neck'' region between separating fission fragments, was a major contributing mechanism.

The experiment utilized the SuperHILAC accelerator facility of the Lawrence Berkeley Laboratory to induce the reaction 856 MeV ^{98}Mo + ^{51}V → ^{149}Tb*, an entrance channel not previously studied. We were interested in measuring the coincidences and correlations between fission fragments (FF) and IMFs, neither of which had large production cross sections. Hence, to enhance the coincidence efficiency, heavy trigger (fission) fragments were detected in an array of four gas-ionization telescopes (GT), each at 18° to the beam in the forward hemisphere (two in the horizontal plane containing the beam and two in the vertical plane, located above and below the beam). In addition to the GTs, the experiment employed two ''Wedge'' counters, each consisting of five Si stopping detectors spaced at 10° intervals, with a common gas-ionization chamber for ΔE measurements. These counters were placed symmetrically to subtend the angles 38°–78° on either side of the beam in the horizontal plane. Because of the gas ΔE section, these Wedge detectors had rather low detection thresholds, permitting energy spectral and angular distribution measurements of IMF emissions (as well as ^{4}He particles) to be made down to relatively low energies. Each of the output signals from the Wedge counters and the GTs was split and directed to two separate amplifiers operated at high and low gain, respectively. In this manner, the experiment had sufficient dynamic range to record fission fragments, IMFs, and alpha particles in each of the detectors.

Fig. 1 shows representative inclusive energy spectra for Z identified C fragments (Z = 6), observed at three angles. The left panel gives the spectra in the laboratory frame, and the right panel displays the same data after event-by-event transformation to the c.m. frame. These spectra are typical of those observed for other IMFs in this experiment. Examination of Fig. 1 indicates at least two components in the spectra, which we shall denote as ''high energy'' or ''low energy'' groups, respectively. The high energy group is the dominant feature in the spectra, and exhibits c.m. energy invariance with c.m. angle. The low energy group increases in relative magnitude with increasing angle, and decreases rapidly

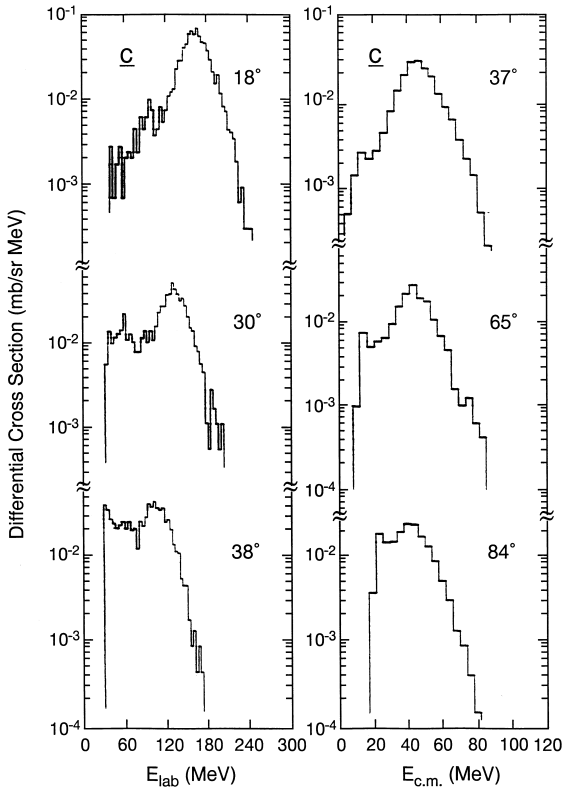

Fig. 1. Representative inclusive energy spectra for Z identified C fragments (Z = 6) observed at three angles as indicated. The left panel gives the spectra in the laboratory frame, and the right panel displays the same data after event-by-event transformation to the c.m. frame.

with increasing Z of the IMF. Most of the observed IMFs are not associated with fission reactions, but those that are come from both the high energy and low energy IMF groups.

In this communication we focus primarily on the IMF-fission coincidence data and the results derived from them using a new analytical technique associated with strongly-reversed kinematics [10,11]. Succeeding publications will present the large body of inclusive IMF data (energy spectra, angular distributions, and cross sections for Z identified IMFs), as well as the ^{4}He-fission coincidence results.

For the current study we selected the entrance channel 856 MeV ^{98}Mo + ^{51}V, which produces the ^{149}Tb composite system at an excitation energy E^{*} = 224 MeV. Reaction-simulation calculations had indicated specific kinematic properties for this chan-

nel, which can be exploited in the present application. The reaction involves strongly-reversed kinematics, which gives rise to two sets of FF energy spectra in a single detector at accessible forward angles, corresponding to the two (unrelated) c.m. emission angles which happen by kinematics to appear at the same laboratory angle but with different energies [10]. The two FF energies ($E_{f1} = 444$ MeV and $E_{f2} = 118$ MeV at 18°) should be easily resolvable in our GT detectors, and at a lab angle of 18° the kinematics determines that the two FF c.m. emission angles are separated by $\sim 90°$. Therefore, coincidence measurements between FF and IMF particles will provide simultaneous observations, in the same detectors, of the correlations with respect to two orthogonal fission axes. This situation is illustrated in Fig. 2, where we present velocity-vector diagrams for fission and IMF emission in the ^{98}Mo + ^{51}V reaction. In these figures, V_c is the velocity of the center-of-mass, and f_1 and f_2 are the velocities of two fission fragments whose c.m. emission angles and energies direct them into the same detector (GT) at 18°. The partner fragments of f_1 and f_2 are undetected, and are represented by the dashed arrows, respectively. Typical IMF velocity vectors are indicated as originating from the center-of-mass (e.g., as a third body accompanying two fission fragments). As the c.m. emission angles of f_1 and f_2 are separated by 90°, it should be possible, by post-experiment software gating on the two FF groups, to compare directly the IMF coincidence rates in appropriately placed detectors for particles emitted along and perpendicular to the scission direction. In effect, one has the ability to rotate the fission axis by 90°, and intensity comparisons can be made in the same detectors, without the additional uncertainties from different detector calibrations.

The three diagrams in Fig. 2 correspond to the three different geometries allowed by our experiment for FF-IMF coincident pairs. In Fig. 2(a), a fission fragment is detected in GT-2 at $-18°$, in coincidence with an IMF in one (or more) of the detectors at 18°, 38°, 48°, 58°, 68°, or 78°. Thus, the FF and IMF are coplanar, and on opposite sides of the beam. By gating on the f_1 signals in GT-2, coincident particles emitted *normal* to the fission axis will be preferentially observed in the more forward IMF detectors, and those emitted *along* the fission direc-

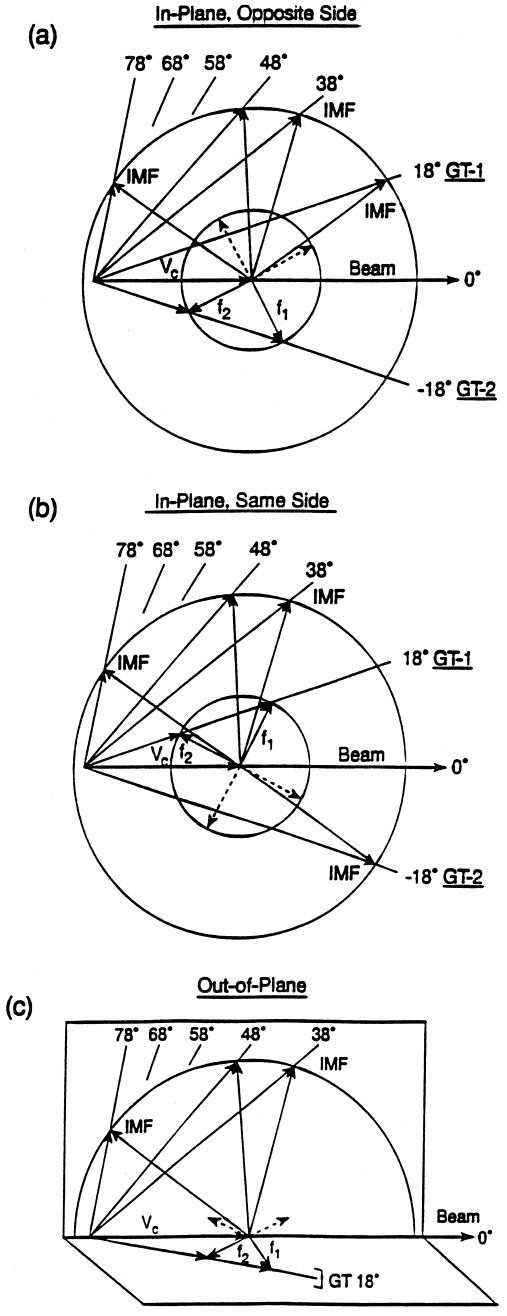

Fig. 2. Vector diagrams indicating expected average emission and detection velocities for first and second solution fission fragments, f_1 and f_2, and IMFs, when (a) the FF and IMF are detected on opposite sides of the beam; (b) the FF and IMF are detected on the same side of the beam; and (c) the FF and IMF are detected in orthogonal planes. The dashed arrows represent the complementary (undetected partner) fission fragments, and the relevant detector angles are indicated.

tion will be favored in the more backward IMF detectors. On the other hand, selection of f_2 signals in GT-2 as the coincidence trigger requirement will enhance *perpendicular* emissions in the more backward IMF detectors, and focus *axial* particle emissions into the more forward detectors. For those IMFs whose emissions are uncorrelated with the FF direction, one would expect rather flat angular distributions for both f_1 and f_2 triggers, since the IMF detectors are all coplanar with the FF trigger detector.

In Fig. 2(b), GT-1 serves as the FF trigger detector, and hence is on the same side of the beam as the IMF detectors. Here detection of f_1 fragments in GT-1 results in coincident particles being directed preferentially backward if they are emitted *normal* to the FF axis, and more forward if emitted *along* the FF axis. Selection of f_2 events in the GT-1 trigger reverses the predictions for *perpendicular* and *axial* emissions. Thus the coincident geometries illustrated in Figs. 2(a) and 2(b) have the effect of interchanging the predictions for IMF intensities associated with the selection of f_1 or f_2 triggers. This provides a very powerful test which can be applied to the experimental IMF/FF coincidence data. Just as in Fig. 2(a), the configuration in Fig. 2(b) predicts flat angular distributions for uncorrelated IMFs, independent of the f_1 or f_2 trigger selections.

Finally, the diagram in Fig. 2(c) represents a configuration in which the FF trigger detector is in a plane normal to the IMF detectors. In this geometry, detection of a fission fragment localizes the initial angular momentum of the composite system (prior to fission or particle emission) in the direction normal to the beam and contained in the plane of the IMF detectors. Thus the spin-driven emission of IMFs will have maximum probability at 90° to the spin direction, and will decrease monotonically as the angle with respect to the spin decreases [12]. Any correlation between IMF emission and the fission axis will appear superimposed on this distribution, and should be detectable as differences associated with the f_1 or f_2 trigger selections.

Let us now consider the experimental data. In this experiment we have arbitrarily taken IMFs to be fragments with Z in the range 3–23, and have operationally defined the fission fragment region to be Z = 24–40. (It should be noted, however, that there is no discontinuity in crossing from one region into the other.) For the ^{98}Mo + ^{51}V reaction studied here, we measured inclusive (integrated) cross sections to be 442 ± 40 mb for fission and 274 ± 25 mb for IMF production [13]. For comparison, the inclusive (integrated) ^{4}He emission cross section is 1172 ± 59 mb. The Z-identified IMFs exhibited inclusive angular distributions and energy spectra characteristic of statistical emissions from an equilibrated source [13]. The coincidence measurements between IMFs and fission fragments comprise a data set which represents a subset of reactions in which at least three significant bodies are present in the final state - a detected IMF, a detected fission fragment, and an undetected fission fragment. The total (integrated) IMF/fission coincidence yield was determined as 44.2 ± 9.7 mb. This means that 44.2 ± 9.7 mb of IMF production (Z = 3–23) is in association with 442 ± 40 mb of fission (Z = 24–40), or, on average, there is 0.10 ± 0.02 IMF produced per fission decay. Comparing the derived IMF yield associated with fission to the inclusive IMF yield, we see that only about 16% of the IMF production is fission related, implying that the bulk (84%) of IMFs originate in reactions which do not lead to two ''normal'' fission fragments along with the IMF. (These latter IMFs result from binary fragmentation processes of evaporation-like or asymmetric-fission-like character [13].) It is, however, the 16% of fission-associated IMFs that we shall focus on here.

The experimental IMF/fission coincidence results are shown in Fig. 3. Each part of this figure, (a), (b), and (c), presents data derived, respectively, from the corresponding configuration represented in Fig. 2. In Fig. 3(a) we give the IMF multiplicity (the IMF-fission cross section divided by the fission singles cross section at the same trigger angle) as a function of the IMF c.m. angle. The fission fragment trigger angle was 18°, in the same plane as the IMF detectors, but on the opposite side of the beam. The filled and open squares are, respectively, the IMF multiplicities gated by first and second fission-fragment solutions in the trigger detector. Because the absolute differential cross sections for first and second fragment solutions are very different, it is necessary to compare *multiplicities* to have the two data sets on an equal footing. In Fig. 3(b), the data representation is the same, except that the fission-

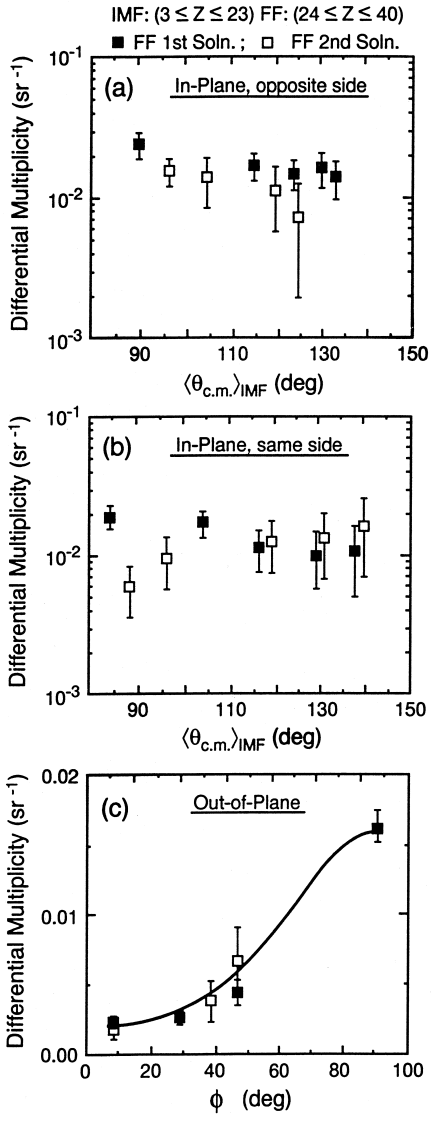

Fig. 3. Experimentally measured IMF-FF angular correlations for the three detector configurations represented by the corresponding vector diagrams in Fig. 2. The IMF-fission coincidences triggered by first and second FF solutions are indicated by filled and open data points, respectively. The error bars are statistical only.

fragment trigger detector is now on the same side of the beam as the IMF detectors. In these figures, average c.m. angles were determined on an event-by-event basis by first transforming individual lab velocities and then averaging the derived c.m. angles. Data from the 78° (lab) detectors have not been included, since very few events were observed at this kinematically restricted angle.

From the results in Figs. 3(a) and 3(b), we may draw two important conclusions. First, the excellent agreement in IMF multiplicities between the open and filled points, corresponding to the two fission-fragment solutions with very different Jacobians, strongly indicates that our analysis and implementation of the double-solution trigger technique has been carried out correctly. Secondly, within the statistical uncertainties of the present data sets, there are no distinguishable differences between IMF multiplicities gated by first and second solution fission-fragment triggers. This implies the absence of a significant correlation between IMF emission direction and the fission axis.

Fig. 3(c) shows the IMF-fission correlation for a FF trigger at 18° to the beam, but in a plane perpendicular to the IMF detectors, as represented by the diagram in Fig. 2(c). The angle ϕ is the IMF detection angle with respect to the initial spin of the system (as determined by the trigger detector). The IMF-fission coincidences triggered by first and second FF solutions are indicated by filled and open data points, respectively. The solid curve is a theoretically predicted function (based upon the statistical model), fitted to the data, and involves no correlation between IMF and FF directions other than that arising from the initial spin direction [12]. The excellent agreement between the calculation and both sets of coincidence data strongly suggests that most of the IMF emission associated with fission reactions occurs prior to the fission act itself, and therefore has no relation to the specific fission-axis direction. One should note that this conclusion from the comparison in Fig. 3(c), while in agreement with that drawn from Figs. 3(a) and 3(b), is essentially based on an independent argument.

Several studies have reported measurements of IMFs in association with fission [5,14–17]. Some of these involved highly fissionable targets bombarded with light projectiles [15–17], leading to a distribution of initial excitation energies, while others focussed on peripheral collisions between two heavy nuclei [14]. While these experiments observed IMFs both correlated and uncorrelated with the fission axes, the IMF yields were much smaller than in the present work and originate in reactions which are

quite different, even though the excitation energies may be comparable. Studies of symmetric systems at substantially higher energies [18,19] have associated three body events with sequential fission following a binary deep-inelastic interaction. In the ^{98}Mo + ^{51}V reaction studied here ($E/A = 8.7$ MeV), complete fusion is essentially a requisite for the occurrence of fission, due to the strong dependence of fission probability on nuclear charge in this mass and energy region. A more closely related investigation is that of the ^{86}Kr + ^{63}Cu reaction [5], which produced the same compound nucleus, ^{149}Tb, at $E^* = 194$ MeV. In that work, the analyses of inclusive IMF spectra compared to coincidence spectra suggested the major IMF yield originated in two-body (non-fission-associated) breakup, with a second pathway corresponding to IMF ejection followed by sequential fission. Our present results derived via a different technique and arguments, are in excellent agreement with these conclusions from [5]. However, we find no evidence from Fig. 3(c) to support a pathway of simultaneous three-body breakup, as has been suggested [5] for the low energy group component in the IMF spectra. It is also noteworthy that the IMF inclusive cross sections are very similar in the two studies, indicating a significant independence of entrance-channel asymmetry.

Acknowledgements

We greatly appreciate the efforts of Paul De Young of Hope College, in providing guidance and assistance in the data analysis. Bill Rathbun of LBL was very helpful with the data acquisition system, and the LBL SuperHILAC staff delivered a stable and intense ^{98}Mo beam. This project was supported by the Division of Nuclear Physics, US Department of Energy.

References

[1] W.E. Parker, M. Kaplan, D.J. Moses, J.M. Alexander, J.T. Boger, R.A. Lacey, D.M. de Castro Rizzo, Nucl. Phys. A 568 (1994) 633.
[2] W.E. Parker, M. Kaplan, D.J. Moses, J.M. Alexander, R.A. Lacey, D.M. de Castro Rizzo, J. Boger, A. Narayanan, G.F. Peaslee, D.G. Popescu, Nucl. Phys. A 594 (1995) 1.
[3] J. Boger, J.M. Alexander, G. Auger, A. Elmaani, S. Kox, R.A. Lacey, A. Narayanan, M. Kaplan, D.J. Moses, M.A. McMahan, P.A. DeYoung, C.J. Gelderloos, G. Gilfoyle, Phys. Rev. C 49 (1994) 1576.
[4] J. Boger, J.M. Alexander, A. Elmaani, S. Kox, R.A. Lacey, A. Narayanan, D.J. Moses, M.A. McMahan, P.A. DeYoung, C.J. Gelderloos, Phys. Rev. C 49 (1994) 1597.
[5] J. Boger, S. Kox, G. Auger, J.M. Alexander, A. Narayanan, M.A. McMahan, D.J. Moses, M. Kaplan, G.P. Gilfoyle, Phys. Rev. C 41 (1990) R801.
[6] N. Carjan, M. Kaplan, Phys. Rev. C 45 (1992) 2185.
[7] M. Kaplan, W.E. Parker, D.J. Moses, E. Vardaci, J.M. Alexander, J. Boger, R. Lacey, N. Carjan, in: W. Bauer, J. Kapusta (Eds.), Advances in Nuclear Dynamics, World Scientific Co. Publishing, Singapore, 1991, p. 8.
[8] R. Lacey, N.N. Ajitanand, J.M. Alexander, D.M. de Castro Rizzo, G.F. Peaslee, L.C. Vaz, M. Kaplan, M. Kildir, G. La Rana, D.J. Moses, W.E. Parker, D. Logan, M.S. Zisman, P. DeYoung, L. Kowalski, Phys. Rev. C 37 (1988) 2540.
[9] R. Lacey, N.N. Ajitanand, J.M. Alexander, D.M. de Castro Rizzo, G.F. Peaslee, L.C. Vaz, M. Kaplan, M. Kildir, G. La Rana, D.J. Moses, W.E. Parker, D. Logan, M.S. Zisman, P. DeYoung, L. Kowalski, Phys. Rev. C 37 (1988) 2561.
[10] M. Kaplan, W.E. Parker, D.J. Moses, R. Lacey, J.M. Alexander, Nucl. Instr. Methods in Phys. Res. A 327 (1993) 551.
[11] D.J. Moses, M. Kaplan, J.M. Alexander, D. Logan, M. Kildir, L.C. Vaz, N.N. Ajitanand, E. Duek, M.S. Zisman, Z. Physik A 320 (1985) 229.
[12] G.L. Catchen, M. Kaplan, J.M. Alexander, M.F. Rivet, Phys. Rev. C 21 (1980) 940.
[13] E. Vardaci, M. Kaplan, W.E. Parker, D.J. Moses, J.T. Boger, G.J. Gilfoyle, M.A. McMahan, to be published.
[14] J. Tõke, B. Lott, S.P. Baldwin, B.M. Quednau, W.U. Schröder, L.G. Sobotka, J. Barreto, R.J. Charity, D.G. Sarantites, D.W. Stracener, R.T. de Souza, Phys. Rev. Lett. 75 (1995) 2920, and references therein.
[15] S.L. Chen, R.T. de Souza, E. Cornell, B. Davin, T.M. Hamilton, D. Hulbert, K. Kwiatkowski, Y. Lou, V.E. Viola, R.G. Korteling, J.L. Wile, Phys. Rev. C 54 (1996) R2114.
[16] D.E. Fields, K. Kwiatkowski, K.B. Morley, E. Renshaw, J.L. Wile, S.J. Yennello, V.E. Viola, Phys. Rev. Lett. 69 (1992) 3713.
[17] R. Yanez, T.A. Bredeweg, E. Cornell, B. Davin, K. Kwiatkowski, V.E. Viola, R.T. de Souza, R. Lemmon, R. Popescu, Phys. Rev. Lett. 82 (1999) 3585.
[18] G. Casini, P.G. Bizzeti, P.R. Maurenzig, A. Olmi, A.A. Stefanini, J.P. Wessels, R.J. Charity, R. Freifelder, A. Gobbi, N. Herrmann, K.D. Hildenbrand, H. Stelzer, Phys. Rev. Lett. 71 (1993) 2567.
[19] A.A. Stefanini, G. Casini, P.R. Maurenzig, A. Olmi, R.J. Charity, R. Freifelder, A. Gobbi, N. Herrmann, K.D. Hildenbrand, M. Petrovici, F. Rami, H. Stelzer, J.P. Wessels, M. Gnirs, D. Pelte, J. Galin, D. Guerreau, U. Jahnke, A. Peghaire, J.C. Adloff, B. Bilwes, R. Bilwes, G. Rudolf, Z. Phys. A 351 (1995) 167.